

This is a repository copy of *QM/MM studies into the H₂O₂-dependent activity of lytic polysaccharide monooxygenases: Evidence for the formation of a caged hydroxyl radical intermediate*.

White Rose Research Online URL for this paper:

<https://eprints.whiterose.ac.uk/126185/>

Version: Accepted Version

Article:

Wang, Binju, Johnston, Esther M., Li, Pengfei et al. (4 more authors) (2018) QM/MM studies into the H₂O₂-dependent activity of lytic polysaccharide monooxygenases: Evidence for the formation of a caged hydroxyl radical intermediate. *ACS Catalysis*. 1346–1351. ISSN 2155-5435

<https://doi.org/10.1021/acscatal.7b03888>

Reuse

Items deposited in White Rose Research Online are protected by copyright, with all rights reserved unless indicated otherwise. They may be downloaded and/or printed for private study, or other acts as permitted by national copyright laws. The publisher or other rights holders may allow further reproduction and re-use of the full text version. This is indicated by the licence information on the White Rose Research Online record for the item.

Takedown

If you consider content in White Rose Research Online to be in breach of UK law, please notify us by emailing eprints@whiterose.ac.uk including the URL of the record and the reason for the withdrawal request.

QM/MM studies into the H₂O₂-dependent activity of *lytic polysaccharide monooxygenases*: evidence for the formation of a caged hydroxyl radical intermediate

Binju Wang[†], Esther M. Johnston[‡], Pengfei Li[‡], Sason Shaik[§], Gideon J. Davies[#], Paul H. Walton[‡], Carme Rovira^{†,&,*}

[†]Departament de Química Inorgànica i Orgànica & IQTCUB, Universitat de Barcelona, Martí i Franquès 1, 08028 Barcelona, Spain. [‡]Department of Chemistry, University of York, Heslington, YO10 5DD, UK. [§]Department of Chemistry, University of Illinois at Urbana–Champaign, Urbana, Illinois 61801, USA. [#]Institute of Chemistry, The Hebrew University of Jerusalem, Givat Ram Campus, 91904 Jerusalem, Israel. [¶]York Structural Biology Laboratory, Department of Chemistry, University of York, Heslington, YO10 5DD, UK. [&]Institució Catalana de Recerca i Estudis Avançats (ICREA), Passeig Lluís Companys, 23, 08020 Barcelona, Spain.

ABSTRACT: Lytic polysaccharide monooxygenases (LPMOs) are promising enzymes for the conversion of lignocellulosic biomass into biofuels and biomaterials. Classically considered oxygenases, recent work suggests that H₂O₂ can, under certain circumstances, also be a potential substrate. Here we present a detailed mechanism of the activation of H₂O₂ by a C4-acting LPMO using small model DFT and QM/MM calculations. Our calculations show that there is an efficient mechanism to break the O-O bond of H₂O₂, with a low barrier of 5.8 kcal/mol via a one electron transfer from the LPMO-Cu(I) site to form an HO• radical, stabilized by hydrogen bonding interactions. QM/MM calculations further show that the H-bonding machinery of the enzyme directs the HO• radical to abstract a hydrogen atom from the Cu(II)-OH rather than from the substrate in what is essentially a caged-radical reaction, thereby forming a Cu(II)-oxyl species. The Cu(II)-oxyl species then exclusively oxidizes the C4-H bond due to the position of the substrate. Our calculations also suggest that the C4-hydroxylated intermediate can be efficiently hydrolyzed in water and this process does not require enzymatic catalysis.

Keywords: LPMO; H₂O₂ activation; QM/MM calculations; HO• radical; cluster-continuum; hydrolysis

Lignocellulosic biomass is an abundant and renewable resource, and it has long been recognized as one of the most promising raw materials for the production of biofuels and biomaterials.^{1,2} However, the recalcitrant nature of lignocellulose impedes its decomposition under mild conditions.¹ Cellulases can break down cellulose into oligosaccharides, but this process is usually inefficient due to the slow depolymerization of crystalline cellulose.^{3,4}

In the last few years, it has been shown that copper-dependent lytic polysaccharide monooxygenases (LPMOs) utilize molecular oxygen and an electron donor to catalyze the oxidative O₂-dependent cleavage of insoluble polysaccharides.⁴⁻⁶ These enzymes first depolymerize cellulose through hydroxylation of the C1 or C4 position of the scissile glycosidic bonds, and the subsequent elimination leads to the cleavage of the glycosidic bond, resulting in aldonic acids or 4-keto sugars at oxidized chain ends.⁵⁻⁶ Despite their industrial importance and extensive experimental studies, the nature of the active species and the detailed mechanism of action of these enzymes remains elusive.⁴⁻⁶ The active site of the LPMO contains a mononuclear copper center ligated by two His ligands (methylated His1 and His78), an arrangement known as the histidine brace. Various active species

have been proposed for the activity of LPMOs, including a Cu(II)-superoxide,^{4,5d,7} a Cu(III)-OH^{6c,8} and a Cu(II)-oxyl^{4,6c,9,10}, but none of these has been characterized or observed spectroscopically. Previous theoretical calculations on small enzyme models have shown that a Cu(II)-superoxide species is a relatively poor oxidant for C-H activation compared with Cu(II)-oxyl species,¹⁰ but subsequent QM/MM calculations¹¹ suggested that the protein environment could significantly affect the structure and the coordination environment of a Cu(II)-superoxide species. Recent experimental work proposed that hydrogen peroxide can also be an active co-substrate in LPMO catalysis in the presence of a substoichiometric amount of reducing agent, in which the oxidant was proposed to be a hydroxyl radical formed after reductive cleavage of the O-O bond.¹² This work dovetails into the observation that LPMOs can generate H₂O₂ from uncoupled turnover when exposed to O₂ and a reducing agent in the absence of a substrate.^{6d,13,14} This dual dependence on co-substrates has been observed in some other metalloenzymes, such as the Fe(II)-dependent (S)-2-hydroxypropylphosphonic (S-HPP) acid epoxidase (HppE), in which O₂ can be reduced to H₂O₂ in the presence of external reductants, converting HppE to a H₂O₂-dependent peroxidase.^{15,16}

Motivated by these observations, we were drawn to investigate the H₂O₂-dependent activation mechanism of the LPMOs, both as part of a wider mechanism in which the production of peroxide from O₂ and a reducing agent is catalyzed by the LPMO, and also via the direct addition of peroxide. Herein we reveal the mechanism of action of the LPMOs in the presence of H₂O₂ using a combination of small model DFT calculations, classical molecular dynamics (MD) simulations, and quantum mechanical/molecular mechanical (QM/MM) calculations, which yield atomistic information about the structures and mechanisms within the native environment of the protein.¹⁷⁻²⁰ This is a well-tested approach that has been proven reliable for metalloenzymes.²¹ Importantly, we benchmark our calculations on the high resolution crystal structure of a LPMO from *Lentinus similis* (CAZY classification AA9) bound to a polysaccharide, which was recently obtained for the first time (PDB code: 5ACF for the Cu(II) state with cellobiose), and for which Michaelis-Menten kinetics are reported for the site-specific oxidation of the C4-H bond of the oligosaccharide.⁸

To investigate H₂O₂ activation by the LPMOs, a small enzyme model was initially constructed for DFT calculations, using the coordinates of the high-resolution crystal structure with appropriate truncations and constraints (see Figure 1 and Supporting Information). This model was optimized using the hybrid functional

B3LYP, a TZVP basis set on the Cu, ligating atoms, and the His ring atoms, and SVP on the remaining atoms. The resulting structure agrees well with the crystal structure of *Ls(AA9)A* and celotriose in the Cu(I) state (Figure S1A). H₂O₂ was added to the optimized model of the Cu(I) state by replacing the equatorial Cl ligand with H₂O₂. After optimization, the H₂O₂ shifted to bind in the active site pocket 3.50 Å away from the Cu(I) to form hydrogen bonding interactions with Gln162 and the C3-OH of the subsite +1 sugar (Figure S2A). This contrasts with the positioning of H₂O₂ when the model is optimized in the absence of substrate (Figure S2B), in which the distance between Cu(I) and H₂O₂ decreases to 2.86 Å due to hydrogen bonding with Gln162 alone. The difference between the H₂O₂ binding geometries in the presence and absence of substrate highlights the key role of second sphere hydrogen bonding interactions in positioning H₂O₂ in the active site pocket.

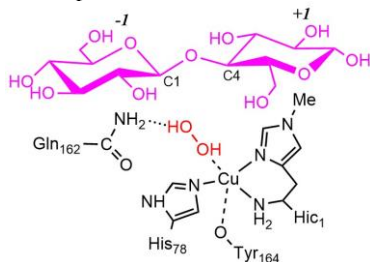


Figure 1. Small active site model and atom labeling used to investigate H₂O₂ activation by the LPMOs.

After optimization of the H₂O₂ position in the small model with substrate, the O-O bond cleavage coordinate was investigated by elongating the O-O bond by fixed 0.1 Å steps (Figure S3), considering three spin surfaces: the two-electron transfer, represented by an S=0 spin restricted ground state, and the one electron transfer in a spin polarized S=0 ground state and the S=1 state. During the reaction, H₂O₂ shifts to be much closer to the Cu(I), similar to the geometry seen in the structure without substrate. On the most favorable spin polarized S=0 ground state surface, the homolytic cleavage of the O-O bond leads to a localized HO• radical and a Cu(II)-OH (Figure S4A), with a ΔE of ~ 7.7 kcal/mol (estimated from the crossing point between the spin restricted and spin polarized ground states, Figure S3). The resulting HO• radical is stabilized by orbital overlap between a filled p orbital on the hydroxide ligand and the empty orbital of the HO• radical (Figure S4B). Additional stabilization is provided by hydrogen bonds from Gln162 and from the C3-OH of the substrate. The proximity of the localized HO• radical to the hydroxide ligand on the Cu(II) opens up the possibility of hydrogen atom abstraction (HAA) from the Cu(II)-OH by the HO• radical to form a Cu(II)-oxyl and H₂O, akin to a ‘caged radical’ reaction. Indeed, a low energy transition state can be found for this process (Figure S5A), with a ΔE^\ddagger of 7.8 kcal/mol and ΔG^\ddagger of 2.8 kcal/mol on the spin polarized singlet surface. The oxyl ligand of the resulting Cu(II)-oxyl species is positioned close to the reactive C4-H bond of the sugar substrate, with an O-H distance of 2.27 Å (Figure S5B). The resulting HAA from the C4-H bond by the Cu(II)-oxyl proceeds with a low ΔE^\ddagger of 9.9 kcal/mol and a ΔG^\ddagger of 7.8 kcal/mol on the triplet surface and a similar barrier on the spin polarized singlet surface.

While these small model calculations suggest that a low energy pathway exists for the activation of H₂O₂ by the Cu(I) site in the LPMOs, leading to substrate oxidation, they may not fully capture all the hydrogen bonding interactions in the active site pocket or the effects of the protein environment. To better describe the hydrogen bonding network, therefore, QM/MM calculations were performed. The Cu(H₂O₂) active site was parameterized using the MCPB.py tool of AMBER.²² After proper setup

(see SI for details), a fully relaxed MD simulation was performed on the fully solvated enzyme complex. A representative snap-shot from the equilibrated system was selected for subsequent QM/MM calculations. We also calculated the most populated structures by clustering of the MD trajectories (see Figure S8), and we can see that the active site structure is well converged and the most populated structure is quite similar to the representative one (Figure S9A) used for QM/MM calculations. The QM region (149 atoms) was described with the hybrid UB3LYP functional at two levels. For the geometry optimizations, the all-electron basis Def2-SVP was used for all atoms (labeled B1). The energies were subsequently corrected using the all-electron TZVP basis set, labeled B2 (see SI).

Figure 2 shows the QM/MM optimized structure of the LPMO-Cu(I)-H₂O₂ complex. As found in the small model, H₂O₂ does not coordinate to the Cu(I), remaining at a distance of 2.77 Å, but the dense H-bonding network involving His78, His147, Gln162 and Glu148 stabilizes and reorients H₂O₂ in the active site. Similar features are observed for Cu(II)-H₂O₂, except that H₂O₂ is coordinated to the metal atom (with a distance of 2.10 Å) and strongly bound in the active site (see Figure S6A). While the Cu(II) state is the resting state of the LPMO active site, the reported experimental reactivity of an LPMO with H₂O₂ requires a reducing agent, suggesting that the Cu(I) state is the state that activates H₂O₂. Indeed, activation of H₂O₂ by the Cu(II) state requires a considerable energy (> 35 kcal/mol) due to the formation of a Cu(III) product (Figure S9B). As such, we further considered only the one electron reduced state, i.e. LPMO-Cu(I)-H₂O₂. Figure 3a shows the QM/MM reaction energy profile starting from the reactant complex (structural details are provided in the SI).

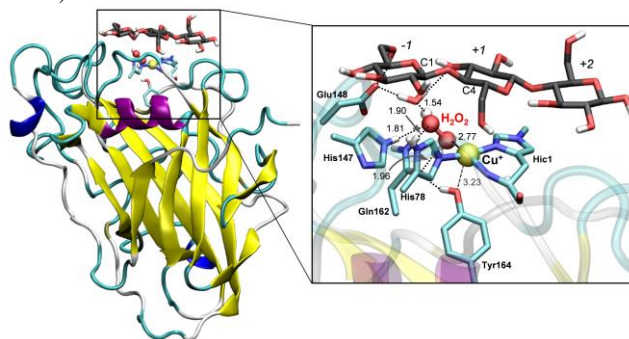


Figure 2. QM/MM optimized structure of the LPMO-Cu(I)-H₂O₂ complex from the representative MD snapshot. Key distances are given in angstroms. Most hydrogen atoms of C-H bonds have been omitted for clarity.

The LPMO-Cu(I)-H₂O₂ complex has a singlet ground state. Starting from the LPMO-Cu(I)-H₂O₂ complex (¹RC1 in Figure 3a), the homolytic O-O bond cleavage via ¹TS1 leads to a Cu(II)-OH species along with an HO• radical (¹IC1 intermediate complex) with a barrier of 5.8 kcal/mol, in accord with the mechanism from the small model DFT studies. Calculations with another snapshot yield a similar barrier for the homolytic O-O bond cleavage (4.7 kcal/mol in Figure S26). The so-generated ¹IC1 exhibits antiferromagnetic coupling of the Cu(II) (with a spin density of -0.56) with the HO• radical (with a spin density of 0.72 at the O atom). Starting from ¹IC1, we considered two competing pathways. The first one (red line in Figure 3a) is the HAA from the closest sugar anomeric carbon (C1, see Figure 3b) by the OH radical, via the ¹TS2 transition state. The competing pathway (black line) is the HAA from the Cu(II)-OH (¹TS3) to generate a Cu(II)-O• species (¹IC3). The HAA from the Cu(II)-OH is favored over HAA from the substrate C1 by 4.9 kcal/mol. As is seen in the small model calculations, it is clear that the LPMO active site directs the Cu(I)-H₂O₂ complex towards the formation of a Cu(II)-O• species by the effective formation of a radical cage.

Consistent with the previous findings,^{16,21d,23} our results show that the hydrogen bond machinery of the enzyme plays a key role in controlling the reactivity and selectivity of H₂O₂ activation. After O-O homolysis, the resulting HO• radical is locked in position by two strong H-bonds with His147 (1.78 Å) and a neighboring water (1.82 Å) that in turn is H-bonded to Gln148 and the sugar C3-OH (Figure 3b). A weaker hydrogen bond with Gln162 (1.92 Å) is also observed. All these indicate that the second coordination sphere plays a vital role in the activity of LPMO.²⁴ In this conformation, the HO• radical is perfectly positioned to abstract a hydrogen atom from the Cu(II)-OH to form the Cu(II)-O• species, while it is unfavorable to abstract a hydrogen atom from the substrate. Moreover, the H-bonding network also prevents the rotation of the nascent HO• radical to form a more “free” and reactive HO• radical (see Figure S24), in contrast to the Fenton-like mechanism proposed by Bissarro et al.¹² The restriction of HO• radical reactivity is reminiscent of the role played by the H-bonding machinery in P450 enzymes^{21d,23}. Indeed, the close presence of the correctly matched substrate, as observed in *Ls*(AA9)A, plays a role in directing the reactivity of the hydroxyl radical towards the Cu(II)-OH unit. Substrates which do not bind as closely to the active site may afford a different reactive pathway in which the hydroxyl radical has greater spatial degrees of freedom, opening up a wider range of sites from which a hydrogen atom can be abstracted.²⁵ Such reactive pathways are potentially deleterious to the enzyme and are at odds with the site-specific oxidations reported for LPMOs. In the resulting Cu(II)-O• species, the O atom bears a high spin density (0.83) and the Cu-O bond is quite long (1.89 Å), suggesting that the Cu(II)-O• is a highly reactive species for C-H activation. As expected, the HAA from the sugar C4 position via ¹TS4 only requires a small barrier of 5.5 kcal/mol. We also considered the HAA from the sugar C1 position starting from ¹IC3, but the process requires a very high energy barrier (21.9 kcal/mol, Figure S25). The high barrier for C1-H activation is mainly caused by the long distance between the C-H bond and the Cu(II)-O• (2.89 Å to the H of C1-H) and an unfavorable conformation for H-abstraction (∠O-H-C1 is 142°). As such, the HAA from C1-H requires significant conformational changes in the substrate and the active site and thus encounters significant barriers. This agrees well with the reported regioselectivity of the *Ls*(AA9)A enzyme, which selectively produces 4-keto sugars, suggesting that the positioning of the substrate is important for regioselective C-H activation.⁸ After HAA, the rebound of the hydroxyl group from the Cu(II)-OH to the C4 radical center of the substrate generates a C4-hydroxylated intermediate (¹IC5). We also tested the triplet surface and it is higher in energy throughout the reaction (Figure S10).

As can be seen from the energy profile in Figure 3a, the overall reaction is quite favorable both kinetically and thermodynamically. Once the H₂O₂ molecule is properly bound in the active site pocket of the LPMO-Cu(I), the reaction will take place very rapidly, leading to substrate hydroxylation. In turnover of *Ls*(AA9)A with O₂ and a fluorescent cellotetraose, the observed *k*_{cat} of 0.11±0.01 min⁻¹ suggests a barrier for the rate-limiting step of ~18 kcal/mol.⁸ Comparing this value to our QM/MM calculations suggests that the reactivity of the LPMO-Cu(I)-H₂O₂ complex is not rate-limiting for LPMO activity.

Other steps such as the reduction of Cu(II) to Cu(I) or hydrolysis of the C4-hydroxylated intermediate are predicted to be the rate-determining step. To determine whether hydrolysis of the C4-hydroxylated intermediate could be the rate-limiting step of turnover, we investigated the hydrolysis of the C4-hydroxylated intermediate in water solution with hybrid cluster-continuum (HCC) model calculations (see SI for more details).²⁶ This model has previously been used to study chemical reactions in aqueous solutions, such as hydration and hydrolysis reactions,²⁷ yielding

thermodynamic properties and mechanistic results comparable to those obtained from more advanced *ab initio* MD simulations.²⁸

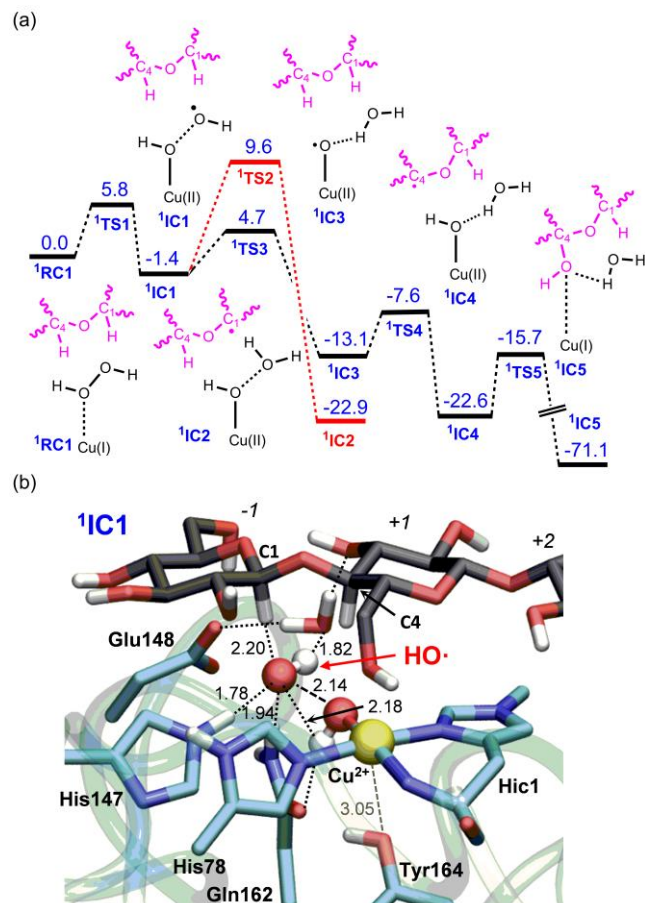


Figure 3. (a) QM/MM (UB3LYP/B2) relative energies (kcal/mol) for the reactivity of the Cu(I)-H₂O₂ complex in the singlet state in the presence of the polysaccharide substrate (pink color). RC = reactant complex, IC = intermediate complex, TS = transition state. (b) Hydrogen bonding network around the OH radical in intermediate ¹IC1.

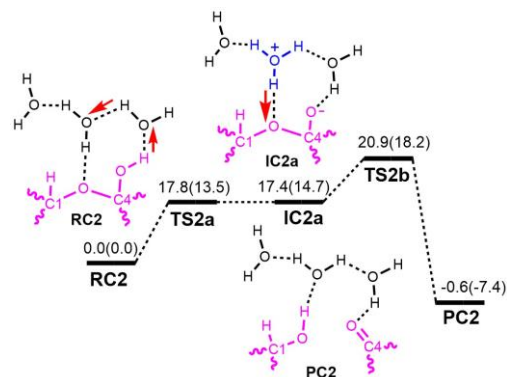


Figure 4. BMK/6-311++G(d,p) relative energies (in kcal/mol) for the hydrolysis of the C4-hydroxylated intermediate in aqueous solution with five explicit water molecules in the HCC calculations, shown along with schematic drawings of key species along the reaction pathway. The relative energies are given as electronic energies first and then free energies in parentheses. The red arrows highlight the direction of proton transfer.

Similar to our previous studies,^{27,28} we constructed a reactant complex of RC2 including water molecules and the substrate that is well connected by a three-dimensional hydrogen bond network.

Figure 4 shows the calculated relative energy profile for the hydrolysis of the C4-hydroxylated intermediate. Starting from the reactant complex (**RC2**), proton transfer from the hydroxyl group at C4, assisted by the adjacent water molecule (**TS2a**), generates an intermediate (**IC2a**) with a H_3O^+ core. The H_3O^+ core is stabilized by strong H-bonding interactions with neighboring water molecules and the glycosidic oxygen, with three H-bonds of 1.41, 1.51 and 1.74 Å (see Figure S27). In **TS2a**, there is one single imaginary frequency of -485.02 i , which corresponds to the vibrational mode of proton transfer, and **TS2a** and **IC2a** are rigorously connected by IRC calculations. It should be noted that the pure proton transfer usually encounters a very small electronic barrier, and such a barrier will be washed out by zero-point motion.²⁹ As such, **TS2a** and **IC2a** are very close in energy. Such findings are in accordance with our previous calculations.^{27,28} The subsequent C4-O bond cleavage via **TS2b**, coupled with proton transfer from the H_3O^+ core to the glycosidic oxygen, results in the 4-ketoaldose hydrolyzed product. The overall reaction requires an energy barrier of 18.2 kcal/mol, consistent with the experimental rate of turnover with O_2 . For comparison, four more explicit water molecules were incorporated into the model of **RC2** to calculate the overall barrier (Figure S28), which leads to an electronic barrier and free energy barrier of 21.6 and 17.1 kcal/mol, respectively, indicating that five explicit water molecules are sufficient to treat the hydrolysis of the glycosidic bond. We also considered the hydrolysis of the C1-hydroxylated intermediate, which has an energy barrier of 14.5 kcal/mol (see Figure S30), indicating the C1-hydroxylated intermediate is even more reactive than the C4-hydroxylated intermediate with respect to the hydrolysis of the glycosidic bond. Clearly, in both C1 and C4-oxidizing LPMOs,³¹ the corresponding hydroxylated intermediates can be efficiently hydrolyzed in water without requiring enzymatic catalysis.

In summary, our small model and QM/MM calculations show that H_2O_2 is efficiently activated by the LPMO-Cu(I) site via a one electron transfer process to form a localized, ‘caged’ $\text{HO}\cdot$ radical. The enzyme H-bonding machinery directs the $\text{HO}\cdot$ radical to abstract the hydrogen atom from the Cu(II)-OH rather than from the substrate, thereby forming a highly reactive Cu(II)-oxyl species. Meanwhile, generation of the, potentially deleterious, free hydroxyl radical $\text{HO}\cdot$, is prevented by the active site H-bond network. Taken together, these calculations suggest that H_2O_2 could be an intermediate in the catalytic cycle of the LPMOs. If O_2 can be reduced to H_2O_2 by the LPMO active site in the presence of external reductants, the LPMO may oxidize substrates by the H_2O_2 -dependent mechanism shown here. The present findings have implications for the engineering of LPMOs toward biomass processing via an H_2O_2 -dependent pathway. Future work will investigate the O_2 activation reaction of the LPMOs and possibility of the formation of H_2O_2 along the reaction coordinate.³⁰

ASSOCIATED CONTENT

Supporting Information

Computational details and Cartesian coordinates of all computed species. This material is available free of charge via the Internet at <http://pubs.acs.org>.

AUTHOR INFORMATION

Corresponding Authors

* Carme Rovira (c.rovira@ub.edu).

ACKNOWLEDGMENT

This work was supported by grants from MINECO (CTQ2014-55174-P to C. R.), AGAUR (2014SGR-987 to C. R.), BBSRC (BB/L021633/1 to PHW,GJD,EMJ, GJD is a Royal Society Ken Murray Research Professor), and National Institute of Health

(Grant GM056207 to P. L.). We acknowledge the computer support provided by the Barcelona Supercomputing Center (BSC-CNS). B. W. thanks AGAUR for a *Beatriu de Pinós* post-doctoral fellowship. P. L. acknowledges the financial support from the National Institute of Health (Grant GM056207).

REFERENCES

- (1) Himmel, M. E.; Ding, S. Y.; Johnson, D. K.; Adney, W. S.; Nimlos, M. R.; Brady, J. W.; Foust, T. D. *Science* **2007**, *315*, 804–807.
- (2) Payne, C. M.; Knott, B. C.; Mayes, H. B.; Hansson, H.; Himmel, M. E.; Sandgren, M.; Ståhlberg, J.; Beckham, G. T. *Chem. Rev.* **2015**, *115*, 1308–1448.
- (3) Wilson, D. B. *Curr. Opin. Biotechnol.* **2009**, *20*, 295–299.
- (4) Beeson, W. T.; Vu, V. V.; Span, E. A.; Phillips, C. M.; Marletta, M. A.; *Annu Rev Biochem* **2015**, *84*, 923–946.
- (5) (a) Harris, P. V.; Welner, D.; McFarland, K. C.; Re, E.; Navarro Poulsen, J. C.; Brown, K.; Salbo, R.; Ding, H.; Vlasenko, E.; Merino, S.; Xu, F.; Cherry, J.; Larsen, S.; Lo Leggio, L. *Biochemistry* **2010**, *49*, 3305–3316. (b) Vaaje-Kolstad, G.; Westereng, B.; Horn, S. J.; Liu, Z.; Zhai, H.; Sorlie, M.; Eijsink, V. G. H. *Science* **2010**, *330*, 219–222. (c) Quinlan, R. J.; Sweeney, M. D.; Lo Leggio, L.; Otten, H.; Poulsen, J.-C. N.; Johansen, K. S.; Krogh, K. B. R. M.; Jørgensen, C. L.; Tovborg, M.; Anthonson, A.; Tryfona, T.; Walter, C. P.; Dupree, P.; Xu, F.; Davies, G. J.; Walton, P. H. *Proc. Natl. Acad. Sci. U.S.A.* **2011**, *108*, 15079–15084. (d) Phillips, C. M.; Beeson, W. T.; Cate, J. H.; Marletta, M. A. *ACS Chem. Biol.* **2011**, *6*, 1399–1406. (e) Beeson, W. T.; Phillips, C. M.; Cate, J. H. D.; Marletta, M. A. *J. Am. Chem. Soc.* **2012**, *134*, 890–892. (f) Hemsworth, G. R.; Henrissat, B.; Davies, G. J.; Walton, P. H. *Nat. Chem. Biol.* **2014**, *10*, 122–126 (g) Lo Leggio, L.; Simmons, T. J.; Poulsen, J. C.; Frandsen, K. E.; Hemsworth, G. R.; Stringer, M. A.; von Freiesleben, P.; Tovborg, M.; Johansen, K. S.; De Maria, L.; Harris, P. V.; Soong, C. L.; Dupree, P.; Tryfona, T.; Lenfant, N.; Henrissat, B.; Davies, G. J.; Walton, P. H. *Nat. Commun.* **2015**, *6*, 5961 (h) Tan, T. C.; Kracher, D.; Gandini, R.; Sygmond, C.; Kittl, R.; Haltrich, D.; Hallberg, B. M.; Ludwig, R.; Divne, C. *Nat. Commun.* **2015**, *6*, 7542. (i) Cannella, D.; Möllers, K. B.; Frigaard, N.-U.; Jensen, P. E.; Bjerrum, M. J.; Johansen, K. S.; Felby, C. *Nat. Commun.* **2016**, *7*, 11134. (j) Vu, V. V.; Beeson, W. T.; Phillips, C. M.; Cate, J. H. D.; Marletta, M. A. *J. Am. Chem. Soc.* **2014**, *136*, 562–565.
- (6) (a) Horn, S. J.; Vaaje-Kolstad, G.; Westereng, B.; Eijsink, V. G. H. *Biochem. Biophys. Res. Commun.* **2012**, *425*, 45. (b) Hemsworth, G. R.; Davies, G. J.; Walton, P. H. *Curr. Opin. Struct. Biol.* **2013**, *23*, 660–668. (c) Walton, P. H.; Davies, G. J. *Curr Opin Chem Biol* **2016**, *31*, 195–207. (d) Vaaje-Kolstad, G.; Forsberg, Z.; Loose, J. S. M.; Bissaro, B.; Eijsink, V. G. H. *Curr. Opin. Struct. Biol.* **2017**, *44*, 67–76. (e) Meier, K. K.; Jones, S. M.; Kaper, T.; Hansson, H.; Koetsier, M. J.; Karkehabadi, S.; Solomon, E. I.; Sandgren, M.; Kelemen, B. *Chem. Rev.* **2017**. DOI: 10.1021/acs.chemrev.7b00421.
- (7) Li, X.; Beeson, W. T.; Phillips, C. M.; Marletta, M. A.; Cate, J. H. *Structure* **2012**, *20*, 1051–1061.
- (8) Frandsen, K. E.; Simmons, T. J.; Dupree, P.; Poulsen, J. N.; Hemsworth, G. R.; Ciano, L.; Johnston, E. M.; Tovborg, M.; Johansen, K. S.; von Freiesleben, P.; Marmuse, L.; Fort, S.; Cottaz, S.; Driguez, H.; Henrissat, B.; Lenfant, N.; Tuna, F.; Baldansuren, A.; Davies, G. J.; Lo Leggio, L.; Walton, P. H. *Nat. Chem. Biol.* **2016**, *12*, 298–303.
- (9) Lee, J. Y.; Karlin, K. D. *Curr Opin Chem Biol* **2015**, *25*, 184–193.
- (10) Kim, S.; Ståhlberg, J.; Sandgren, M.; Paton, R. S.; Beckham, G. T. *Proc Natl Acad Sci USA* **2014**, *111*, 149–154.
- (11) Hedegård, E. D.; Ryde, U. *ACS Omega* **2017**, *2*, 536–545.
- (12) Bissaro, B.; Røhr, Å. K.; Müller, G.; Chylenski, P.; Skaugen, M.; Forsberg, Z.; Horn, S. J.; Vaaje-Kolstad, G.; Eijsink, V. G. H. *Nat. Chem. Biol.* **2017**, *13*, 1123–1128.
- (13) (a) Kittl, R.; Kracher, D.; Burgstaller, D.; Haltrich, D.; Ludwig, R. *Biotechnol Biofuels* **2012**, *5*, 79. (b) Scott, B. R.; Huang, H. Z.; Frickman, J.; Halvorsen, R.; Johansen, K. S. *Biotechnol. Lett.* **2016**, *38*, 425–434.
- (14) Isaksen, T.; Westereng, B.; Aachmann, F. L.; Agger, J. W.; Kracher, D.; Kittl, R.; Ludwig, R.; Haltrich, D.; Eijsink, V. G. H.; Horn, S. J. *J Biol Chem* **2014**, *289*, 2632–2642.
- (15) Wang, C.; Chang, W. C.; Guo, Y. S.; Huang, H.; Peck, S. C.; Pandelia, M. E.; Lin, G. M.; Liu, H. W.; Krebs, C.; Bollinger, J. M. *Science* **2013**, *342*, 991–995.

- (16) Wang, B.; Lu, J.; Dubey, K. D.; Dong, G.; Lai, W. Z.; Shaik, S. *J. Am. Chem. Soc.* **2016**, *138*, 8489–8496.
- (17) Warshel, A. *Angew. Chem., Int. Ed.* **2014**, *53*, 10020–10031.
- (18) Senn, H. M.; Thiel, W. *Angew. Chem., Int. Ed.* **2009**, *48*, 1198–1229.
- (19) Lin, H.; Truhlar, D. G. *Theor. Chem. Acc.* **2007**, *117*, 185–199.
- (20) (a) van der Kamp, M. W.; Mulholland, A. J. *Biochemistry* **2013**, *52*, 2708–2728. (b) Ryde, U. *Curr. Opin. Chem. Biol.* **2003**, *7*, 136–142.
- (21) (a) Kumar, D.; Thiel, W.; de Visser, S. P. *J. Am. Chem. Soc.* **2011**, *133*, 3869–3882. (b) Schyman, P.; Lai, W. Z.; Chen, H.; Wang, Y.; Shaik, S. *J. Am. Chem. Soc.* **2011**, *133*, 7977–7984. (c) Wang, B.; Usharani, D.; Li, C.; Shaik, S. *J. Am. Chem. Soc.* **2014**, *136*, 13895–13901. (d) Wang, B.; Li, C.; Dubey, K. D.; Shaik, S. *J. Am. Chem. Soc.* **2015**, *137*, 7379–7390. (e) A. Li, B. Wang, A. Ilie, K. D. Dubey, G. Bange, I. V. Korendovych, S. Shaik, M. T. Reetz. *Nat. Commun.* **2017**, *8*, 14876.
- (22) (a) Li, P.; Merz Jr, K. M. *J. Chem. Inf. Model.* **2016**, *56*, 599–604. (b) Li, P.; Merz Jr, K. M. *Chem Rev.* **2017**, *117*, 1564–1686.
- (23) Ramanan, R.; Dubey, K. D.; Wang, B.; Mandal, D.; Shaik, S. *J. Am. Chem. Soc.*, **2016**, *138*, 6786–6797.
- (24) Span, E. A.; D. L. M.; Deller, M. C.; Britt, R. D.; Marletta, M. A. *ACS Chem. Biol.*, **2017**, *12*, 1095–1103.
- (25) Simmons, T. J.; Frandsen, K. E. H.; Ciano, L.; Tryfona, T.; Lenfant, N.; Poulsen, J. C.; Wilson, L. F. L.; Tandrup, T.; Tovborg, M.; Schnorr, K.; Johansen, K. S.; Henrissat, B.; Walton, P. H.; Lo Leggio, L.; Dupree, P. *Nature Commun.*, **2017**, *8*, 1064.
- (26) (a) Pliego, J. R.; Riveros, J. M. *J. Phys. Chem. A*, **2001**, *105*, 7241–7247. (b) Sunoj, R. B.; Anand, M. *Phys. Chem. Chem. Phys.* **2012**, *14*, 12715–12736.
- (27) (a) Wang, B.; Cao, Z. *J. Phys. Chem. A* **2010**, *114*, 12918–12927. (b) Wang, B.; Cao, Z. *Angew. Chem., Int. Ed.* **2011**, *50*, 3266–3270. (c) Wang, B.; Cao, Z. *Chem. Eur. J.* **2011**, *17*, 11919–11929. (d) Wang, Y.; Deng, W.; Wang, B.; Zhang, Q.; Wan, X.; Tang, Z.; Wang, Y.; Zhu, C.; Cao, Z.; Wang, G.; Wan, H. *Nat. Commun.* **2013**, *4*, 2141. (e) Wang, B.; Cao, Z.; Sharon, D.; Shaik, S. *ACS Catal.*, **2015**, *5*, 7077–7090.
- (28) Wang, B.; Cao, Z. *J. Comput. Chem.* **2013**, *34*, 372–378.
- (29) Marx, D.; Tuckerman, M. E.; Hutter, J.; Parrinello, M. *Nature* **1999**, *397*, 601–604.
- (30) (a) Kjaergaard, C. H.; Qayyum, M. F.; Wong, S. D.; Xu, F.; Hemsworth, G. R.; Walton, D. J.; Young, N. A.; Davies, G. J.; Walton, P. H.; Johansen, K. S.; Hodgson, K. O.; Hedman, B.; Solomon, E. I. *Proc. Natl. Acad. Sci. U.S.A.* **2014**, *111*, 8797–8802. (b) O'Dell, W. B.; Agarwal, P. K.; Meilleur, F. *Angew. Chem., Int. Ed.* **2017**, *56*, 767–770.

TOC graphic

